ATMOSPHERIC AND OCEANIC SCIENCE LETTERS, 2014, VOL. 7, NO. 5, 417–421

# The Second Decadal Leading Mode of East Asian Summer Monsoon Rainfall

BAO Qing[1] and YU Pei[1,2]

[1] *The State Key Laboratory of Numerical Modeling for Atmospheric Sciences and Geophysical Fluid Dynamics (LASG), Institute of Atmospheric Physics, Chinese Academy of Sciences, Beijing 100029, China*

[2] *University of Chinese Academy of Sciences, Beijing 100049, China*

Received 18 March 2014; revised 9 April 2014; accepted 14 April 2014; published 16 September 2014

**Abstract** The first decadal leading mode of East Asian summer rainfall (EASR) is characterized by rainfall anomalies along the East Asian subtropical rain belt. This study focuses on the second decadal leading mode (2DLM), accounting for 17.3% of rainfall decadal variance, as distinct from the other two neighboring modes of EAMR, based on the state-of-the-art in-situ rainfall data. This mode is characterized by a South-China-wet–Huaihe-River-dry pattern, and is dominated by a quasi-30-yr period. Further analysis reveals the 2DLM corresponds to an enhanced lower-level monsoon jet, an eastward extension of the western North Pacific subtropical high, and a weakened East Asian upper-level westerly jet flow. The Tibetan Plateau surface temperature and Pacific Decadal Oscillation (PDO) are closely linked with the 2DLM. The regressed SST pattern indicates the PDO-like pattern of sea surface temperature anomalies may have a teleconnection relationship with the 2DLM of EASR.

**Keywords:** decadal leading mode, East Asian summer monsoon, Tibetan Plateau, Pacific Decadal Oscillation

**Citation:** Bao, Q., and P. Yu, 2014: The second decadal leading mode of East Asian summer monsoon rainfall, *Atmos. Oceanic Sci. Lett.*, **7**, 417–421, doi:10.3878/j.issn.1674-2834.14.0030.

## 1 Introduction

East Asian summer monsoon rainfall (EASR) influences almost a quarter of the world's population, and the trends in flooding and drought reproduced by EASR's decadal climate variability have deep impacts on the agriculture, economy, and society of the East Asian (EA) regions. To fully understand the decadal climate variability and trend of EASR and the associated circulation anomaly would be of great benefit not only in providing insights into past climate disaster trends, but also near-term decadal climate predictions (Jia et al., 2013).

The major decadal leading mode of EASR has been studied widely. Research has demonstrated that the decadal trend of the EA subtropical rainfall front is the first major decadal leading mode of EASR (e.g., Nitta and Hu, 1996; Gong and Ho, 2002; Hu et al., 2003; Wang et al., 2008). This major decadal pattern of rainfall variability mainly includes two aspects: the intensified Meiyu (called 'Baiu' in Japan and 'Changma' in Korean) rain belt since the 1960s, and the drought trend in North China. This major decadal leading mode of EASR is related to a common climatic phenomenon known as 'southern China flood-northern China drought'. Some studies have pointed out that the climatic drought trend has occurred in some regions of the northwestern Pacific Ocean, and this drought trend also belongs to this major decadal mode of EASR. Thus, the relevant spatial pattern is called the 'sandwich pattern'. Recent studies show that this major leading mode of EASR has intensified since the 1960s, but turned to be the opposite phase in the most recent decade (Xin et al., 2006; Si and Ding, 2013). Some studies have been carried out to investigate the possible reasons and associated mechanisms, and they have reported that the decadal changes of sea surface temperature (SST) of the northwestern Pacific Ocean (Zhou et al., 2009), human-induced aerosols (Menon et al., 2002), and the thermal forcing of the Tibetan Plateau (Bao et al., 2008; Wang et al., 2008) have all contributed to the trend of the EA subtropical rainfall front.

Due to the differences from data sources, methods, and covered domains, the 2nd Decadal Leading Mode (2DLM) of EASR (hereafter shortened to 2DLM-EASR) is usually mixed up with the first major decadal mode of EASR. Yang and Lau (2004) used a singular value decomposition (SVD) method and found the 2nd decadal mode of rainfall over eastern China is characterized by a positive rain belt along the Yangtze River Valley. Using meteorological station rainfall data in China, Ding et al. (2008) and Lei et al. (2011) demonstrated that the 2nd decadal mode of rainfall exhibits a 'tripole rainfall pattern'. However, both of these studies revealed the rainfall anomaly pattern in South China is another distinct leading decadal mode of EASR. This South China pattern of the rainfall anomalous mode has been shown to have had an abrupt change around 1992–94, and an intensified trend (Kwon et al., 2005; Ding et al., 2008). This mode is recognized as an ENSO-related or tropical SST-related mode. Such an abrupt change was confirmed by Liu et al. (2011) with different sources of observational data.

Because of the relative lack of long-term data, it remains unclear whether or not the abrupt change around 1992–94 related with the leading mode of EASR can be taken as a trend-like feature, or is a part of decadal variation. Considering the uncertainties derived from the methods adopted thus far, the domains covered, and the data sources used, there are still some gaps in our understanding of the characteristics of the 2DLM-EASR, the associated circulation anomaly, and the possible mechanism underpinning the variation.

Corresponding author: BAO Qing, baoqing@mail.iap.ac.cn

By using state-of-the-art products of in-situ rainfall datasets over the whole East Asian region, this work aims to answer the following questions: What are the characteristics of 2DLM-EASR and the associated circulation patterns? Does 2DLM-EASR demonstrate a trend-like variation over the recent several decades? Are there any decadal links between 2DLM-EASR and other decadal variabilities?

The remainder of the paper is organized as follows. Section 2 briefly introduces the datasets and methodologies used. Section 3 presents the 2DLM-EASR and corresponding circulation patterns. Section 4 describes the possible links of 2DLM-EASR with other decadal variabilities. Finally, concluding remarks are provided in section 5.

## 2 Datasets and methodology

The observational precipitation data used in this study are from the National Oceanic and Atmospheric Administration's (NOAA) Precipitation Reconstruction over Land (PREC/L) dataset (Chen et al., 2002), covering the period from 1951 to 2013. Based on 17 000 gauge observational stations, the PREC/L precipitation data are interpolated to a global grid of 0.5° latitude and 0.5° longitude, thus covering the domains of PREC/L in East Asia including not only mainland China, but also the Korean Peninsula, Japan, and some islands in the northwestern Pacific Ocean. The other datasets used in this work include: data from 756 gauge observational stations, supplied by the China Meteorological Administration, including 71 meteorological stations datasets across the Tibetan Plateau; monthly National Centers for Environmental Prediction/National Center for Atmospheric Research (NCEP/NCAR) Reanalysis data (Kalnay et al., 1996); the Hadley Centre's SST datasets from the UK Met Office (Rayner et al., 2003); and the Pacific Decadal Oscillation (PDO) index from the University of Washington (http://jisao.washington.edu/pdo), which is defined as the leading principal component of North Pacific monthly SST variability .

In order to obtain the decadal leading modes of EASR, the empirical orthogonal function (EOF) method is adopted. The boreal summer mean (average of June, July, and August) products of the PREC/L precipitation over the past 60 years (covering 1951 to 2013) are used for the EOF analysis. Before the EOF analysis, all precipitation datasets are filtered by pre-processing using the 9-yr running average to achieve the decadal modes. The EOF analysis is carried out by constructing a correlation matrix to eliminate geographical influences. Thus, the eigenvectors (spatial patterns) are guaranteed to be nondimensional.

## 3 The second decadal leading mode of East Asian summer rainfall

By using state-of-the-art long-term precipitation products to approximate all regions over East Asia, the 1DLM of EASR (hereafter shortened to 1DLM-EASR) is first revealed in Fig. 1a. Similar to previous studies (e.g., Hu et al., 2003; Bao et al., 2008), 1DLM-EASR is manifested with a southwest-northeast tilted 'sandwich pattern' or so-called 'tripole rainfall pattern', including the wet phase along the Meiyu in China, Changma in Korea, and Baiu in Japan, and dry phases in North China and the Northwest Pacific extending to the south of Japan, respectively. Instead of a trend-like variation, the time series of the corresponding principal component 1 (PC1) exhibits a quasi-60-yr oscillation feature.

What are the characteristics of 2DLM-EASR. As shown in Fig. 1b, 2DLM-EASR can be clearly identified. This leading mode is characterized by positive rainfall anomalies, mainly in South China and the Okinawa islands, while there is a dry belt along the Huaihe River Valley extending to the south of Japan. Similar to the tilted feature of 1DLM-EASR, the extension of the southwest-northeast tilted pattern of 2DLM-EASR is relatively weak. Statistical analysis shows that the 2DLM-EASR accounts for approximately 17.3% of rainfall decadal variance, which is distinguished by the other two neighboring modes of EASR (Figs. 1a, 1c, and 1d). Different from the theory of an abrupt change or trend-like variation, the time series of the corresponding principal component 2 (PC2) represents a feature of oscillation. Power spectrum analysis of PC2 suggests the dominant frequency period of PC2 is an approximate quasi 30 years, which passes the 95% confidence level (figure not shown). As shown in Fig. 2b, the timing (1992–1994) of the abrupt change (e.g., Kwon et al., 2005; Ding et al., 2008) should be one of the transition phases from the negative pattern to the positive pattern of 2DLM-EASR, and a similar transitional phase also occurs around 1960.

What are the corresponding circulation anomalies of 2DLM-EASR. Based on the NCEP/NCAR reanalysis data, the corresponding circulation anomalies are obtained via regression analysis with the PC2 of 2DLM-EASR. In Fig. 2, the associated circulation anomalies are given in the lower, middle, and upper tropospheric levels. These corresponding circulation anomalies include an enhanced lower-level monsoon jet flow and an anticyclonic anomaly in the Northwest Pacific at 850 hPa (Fig. 2a), an eastward withdrawal of the Northwest Pacific subtropical high at 500 hPa (Fig. 2b), and a weakening of East Asian westerly jet flow at 200 hPa (Fig. 2c). These circulation anomalies are conducive to rainfall anomalies both in South China and along the Huaihe River Valley. In the lower troposphere, the positive phase of 2DLM-EASR is related with the intensified southwestern moisture jet (Fig. 2a), which transfers the moisture from the South China Sea to South China. Thus, the lower moisture jet leads to a positive precipitation anomaly in South China. In the upper troposphere (Fig. 2c), the weakening East Asian westerly jet flow is conducive to convergence, and subsequently leads to subsidence and a dry precipitation anomaly in the Huaihe River Valley.

## 4 Possible links between 2DLM-EASR and other common decadal signals

The prediction or predictability of decadal signals has

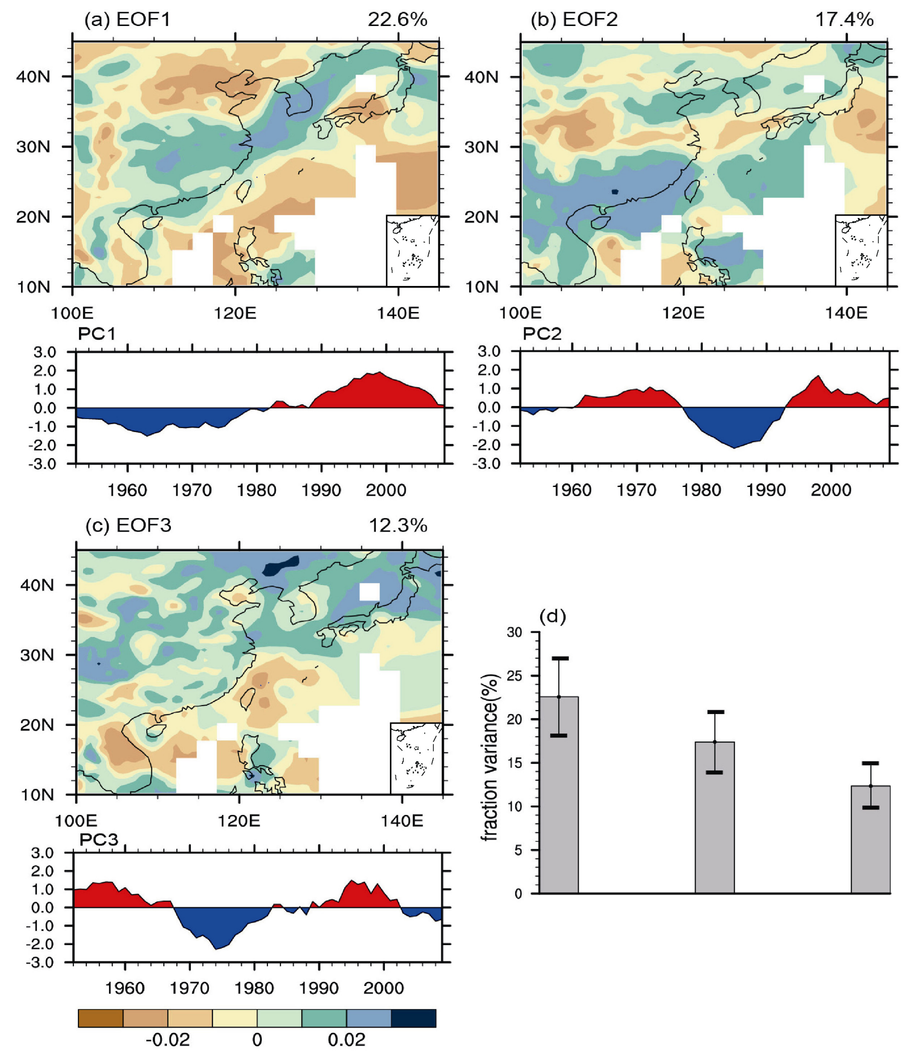


**Figure 1** (a) Spatial pattern and corresponding principal component of the first EOF mode of the 9-yr running mean summer (JJA) precipitation in the East Asian (EA) domain (10–45°N, 100–145°E). (b) and (c) are the same as (a), except for the second and third decadal modes. The fractional variances of these EOF modes are 22.6%, 17.4%, and 12.3%, respectively. All values are nondimensional as the modes are derived from a correlation coefficient matrix. (d) Percentage variance explained by the three leading EOF modes. The short black bars denote error ranges of each mode.

been of great concern in the climate community; thus, it would be of great benefit if we can elucidate the possible linkage between 2DLM-EASR and other common decadal signals. One major and decadal signal is PDO (Latif and Barnett, 1994; Zhang et al., 1997). Another, occurring over East Asia, is the thermal status of the Tibetan Plateau (TP), since the TP is located upstream of the East Asian summer monsoon (Duan and Wu, 2008; Si and Ding, 2013).

Is there any significant correlation between 2DLM-EASR and these other decadal variabilities? Figure 3 presents the time series of the PC2 of 2DLM-EASR, the 9-yr running average thermal status of the TP, and the PDO index from 1951 to 2013. Among these, the thermal status of the TP is represented by the boreal summer mean (TP_TS_JJA (June, July, and August)) and spring mean (TP_TS_MAM (March, April, and May)) of the skin temperature from 71 meteorological stations over the TP. The correlation coefficients between PC2 and TP_TS_JJA, between PC2 and TP_TS_MAM, and between PC2 and PDO, are 0.684, 0.636, and −0.567, respectively, and all of them pass the 97% confidence level. Correlation coefficient analyses suggest that both the thermal status of the TP and the signals of the PDO show a close relationship with the variation of 2DLM-EASR.

Figure 4 is the regressed pattern of SST with the PC2 of 2DLM-EASR. As illustrated, there are three key significant regions in the regressed SST pattern. In the Northern Hemisphere, the largest significant signal comes from the northern Pacific Ocean, which is consistent with the high correlation coefficient of the PDO. In this regard, 2DLM-EASR is considered to have a teleconnection relationship with the PDO. Thus, the predictability of 2DLM-EASR may benefit from this relationship. In the Southern Hemisphere, there are two significant regions detected: one located in the southwestern midlatitude Pacific Ocean, and the other in the southern midlatitude Indian Ocean.

## 5 Summary and concluding remarks

This study focuses on the second decadal leading mode

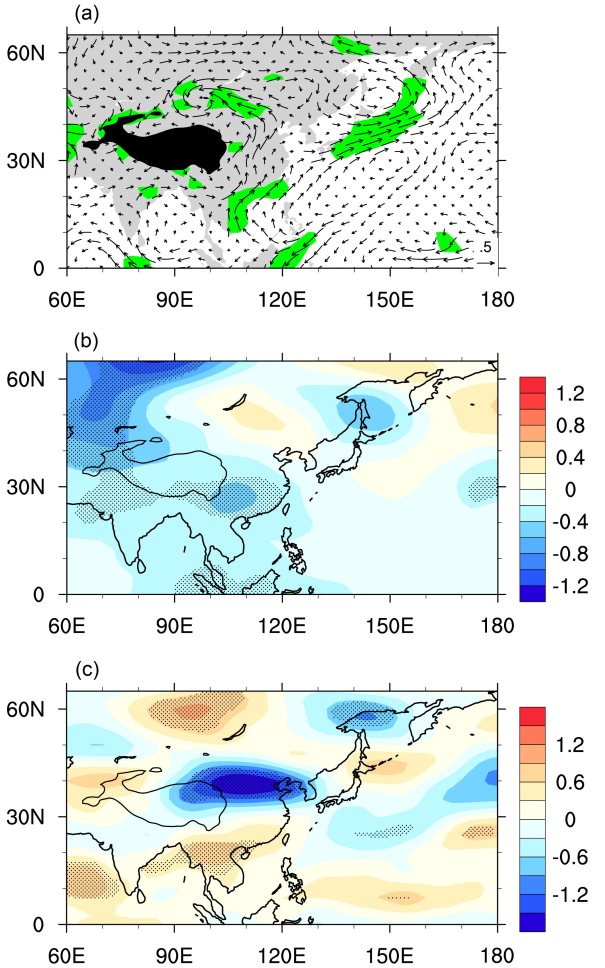


**Figure 2** Atmospheric circulation anomalies regressed with the principal component (PC) of 2DLM-EASR: (a) winds at 850 hPa (vectors; units: m $s^{-1}$); (b) geopotential height at 500 hPa (units: 10 gpm); and (c) zonal winds at 200 hPa (units: m $s^{-1}$). The green colored regions in (a) and the dotted regions in (b) and (c) exceed the 95% confidence level. The black shaded areas in (a) and the bold black lines in (b) and (c) denote TP areas with elevations over 2500 m.

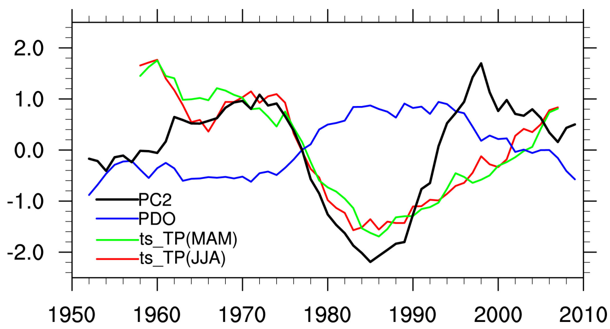


**Figure 3** Time series of the 9-yr running mean MAM (green) and JJA (red) 0-cm skin temperature over the TP, the PDO index (blue), and the principal component of the second mode (PC2) in Fig. 1b (black).

of EAMR, accounting for 17.3% of rainfall decadal variance, as distinct from the other two neighboring modes, based on state-of-the-art in-situ rainfall data. EOF, power spectral analysis, and statistical analysis are used to obtain the characteristics and associated circulation anomalies of 2DLM-EASR. This mode is characterized by a South-

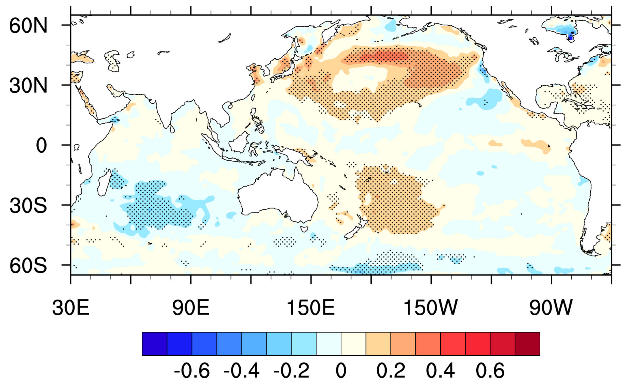


**Figure 4** JJA sea surface temperature anomalies regressed with reference to PC2. The dotted areas indicate significant values above the 95% confidence level.

a quasi-30-yr period. Using reanalysis data, the associated circulation anomalies of 2DLM-EASR are found, which include enhanced lower-level monsoon jet flow, an anticyclonic anomaly near the Northwest Pacific Ocean in the lower troposphere, an eastward withdrawal of the Northwest Pacific subtropical high, and a weakening of the East Asian westerly jet flow at 200 hPa. Correlation analysis suggests that TP surface skin temperature and the PDO are closely linked with the 2DLM. The regressed SST pattern indicates that the PDO-like pattern of SST anomalies may have a teleconnection relationship with 2DLM-EASR. However, the possible underlying physical mechanisms between 2DLM-EASR and the PDO or PDO-like pattern are still unknown. Further studies should be carried out to investigate this issue using numerical modeling via sensitivity experiments with a climate system model.

**Acknowledgements.** This study was supported by the National Basic Research Program (973 Program, Grant No. 2012CB417203), the R&D Special Fund for Public Welfare Industry (Meteorology) (Grant No. GYHY201406001), Strategic Leading Science Projects of the Chinese Academy of Sciences (Grant No. XDA11010402), and the National National Science Foundation of China (Grant Nos. 91337110 and 40805038).

## References

Bao, Q., B. Wang, Y. M. Liu, et al., 2008: The impact of the Tibetan Plateau warming on the East Asian summer monsoon—A study of numerical simulation, *Chinese J. Atmos. Sci.* (in Chinese), **32**(5), 997–100.

Chen, M., P. Xie, J. E. Janowiak, et al., 2002: Global land precipitation: A 50-yr monthly analysis based on gauge observations, *J. Hydrometeorol.*, **3**, 249–266.

Ding, Y. H., Z. Y. Wang, and Y. Sun, 2008: Inter-decadal variation of the summer precipitation in China and its association with decreasing Asian summer monsoon. Part I: Inter-decadal variability of the summer precipitation in China and associated large-scale circulation features, *Int. J. Climatol.*, **28**, 1139–1161, doi:10.1002/joc.1615.

Duan, A. M., and G. X. Wu, 2008: Weakening trend in the atmospheric heating source over the Tibetan Plateau during recent decades. Part I: Observations, *J. Climate*, **21**, 3150–3164.

Gong, D. Y., and C. H. Ho, 2002: Shift in the summer rainfall over the Yangtze River valley in the late 1970s, *Geophys. Res. Lett.*, **29**, 781–784, doi:10.1029/2001GL014523.

Hu, Z. Z., S. Yang, and R. G. Wu, 2003: Long-term climate variations in China and global warming signals, *J. Geophys Res.*, **108**(D19), 4614, doi:10.1029/2003JD003651.

Jia, X. J., J. Y. Lee, H. Lin, et al., 2013: Interdecadal change in the northern hemisphere seasonal climate prediction skill. part I: The leading forced mode of atmospheric circulation, *Climate Dyn.*, doi:10.1007/s00382-013-1988-1.

Kalnay, E., M. Kanamitsu, R. Kistler, et al., 1996: The NCEP/NCAR 40-year reanalysis project, *Bull. Amer. Meteor. Soc.*, **77**, 437–471.

Kwon, M. H., J. G. Jhun, B. Wang, et al., 2005: Decadal change in relationship between East Asia and WPN summer monsoons, *Geophys. Res. Lett.*, **32**, L16709, doi:10.1029/2005GL023026.

Latif, M. and T. P. Barnett, 1994: Causes of decadal climate variability over the north Pacific and North America, *Science*, **266**, 634–637.

Lei, Y. H., B. Hoskins, and J. Slingo, 2011: Exploring the Interplay between natural decadal variability and anthropogenic climate change in summer rainfall over China. Part I: Observational evidence, *J. Climate*, **24**, 4584–4599.

Liu, Y., G. Huang, and R. H. Huang, 2011: Interdecadal variability of summer rainfall in Eastern China detected by the Lepage test, *Theor. Appl. Climatol.*, **106**, 481–488, doi:10.1007/s00704-011-0442-8.

Menon, S., J. Hansen, L. Nazarenko, et al., 2002: Climate effects of black carbon aerosols in China and India, *Science*, **297**, 2250–2253.

Nitta, T., and Z. Z. Hu, 1996: Summer climate variability in China and its association with 500-hPa height and tropical convection, *J. Meteor. Soc. Japan*, **74**, 425–445.

Rayner, N. A., D. E. Parker, E. B. Horton, et al., 2003: Global analyses of sea surface temperature, sea ice, and night marine air temperature since the late nineteenth century, *J. Geophys. Res.*, **108**, D14407, doi:10.1029/2002JD002670.

Si, D., and Y. H. Ding, 2013: Decadal change in the correlation pattern between the Tibetan Plateau winter snow and the East Asian summer precipitation during 1979–2011, *J. Climate*, **26**, 7622–7634.

Wang, B., Q. Bao, B. Hoskins, et al., 2008: Tibetan Plateau warming and precipitation changes in East Asia, *Geophys. Res. Lett.*, **35**, L14702, doi:10.1029/2008GL034330.

Xin, X. G., R. C. Yu, T. J. Zhou, et al., 2006: Drought in late spring of South China in recent decades, *J. Climate*, **19**, 3197–3206.

Yang, F. L., and K. M. Lau, 2004: Trend and variability of China precipitation in spring and summer: Linkage to sea-surface temperatures, *Int. J. Climatol.*, **24**, 1625–1644.

Zhang, Y., J. M. Wallace, and D. S. Battisti, 1997: ENSO-like interdecadal variability: 1900–93, *J. Climate*, **10**, 1004–1020.

Zhou, T. J., R. Yu, J. Zhang, et al., 2009: Why the Western Pacific Subtropical High has extended westward since the late 1970s, *J. Climate*, **22**, 2199–2215.